ParCFD2022
33^{rd} International Conference on Parallel Computational Fluid Dynamics
May 25-27 2022, Alba Italy

AN ADAPTIVE PARALLEL LBM SOLVER FOR HIGH-RESOLUTION AERODYNAMICS AND AEROACOUSTIC

Mikaël GRONDEAU* **AND Ralf DEITERDING†**

Aerodynamics and Flight Mechanics Research Group, University of Southampton,
Boldrewood Innovation Campus, Southampton SO16 7QF, United Kingdom
e-mail: * m.p.grondeau@soton.ac.uk, † r.deiterding@soton.ac.uk

Key words: LBM, Turbulence, LES, wall model, aerodynamics, aeroacoustic

Abstract. AMR-LBM-LES simulations are carried out using our in-house parallel software AMROC. It is first successfully used to calculate the aeroacoustic of a 3D airfoil with wall-resolved simulations. To extend the capability of the software, the implementation of an existing wall model is then validated for a 2D airfoil.

1 INTRODUCTION

Machines like wind turbines are producing an increasing share of our energy needs. It is thus of major importance to study the efficiency, reliability and potential sound-related nuisance of such devices. For this purpose, a high-fidelity CFD tool able to predict the behaviour of turbines at low Mach numbers and high Reynolds numbers is of particular interest. Here, we propose a novel approach to predict the flow and noise around airfoils in a wind-turbine context. This approach is based on the lattice Boltzmann method (LBM).

The LBM is implemented into our in-house parallel software AMROC and is used with adaptive mesh refinement (AMR), which increases the accuracy of simulations and reduces computational costs. Results from wall-resolved simulations of a 3D airfoil in an aeroacoustic context are first presented. Then, to extend the capability of our software, a wall function boundary layer model for the Cartesian ghost-cell approach [1] has been implemented and we present its validation for a 2D airfoil.

The collision operator used in the simulations presented afterwards is the recursive-regularized Bathnagar-Groos-Krook (BGK) collision operator, see [2] for details. The stencils used are the D3Q27 and D2Q9. The employed LES model is the constant coefficient Smagorinsky model. For the calculation of the filtered strain rate tensor we have adopted the "consistent strain" approach by Malaspinas & Sagaut [3].

2 Aeroacoustic simulation of 3D airfoil

The capacity of our numerical method to predict the noise emitted by the flow over a smooth airfoil through direct noise computation is tested. The case is a 3D NACA0012 airfoil at Reynolds number $500,000$ and Mach number 0.22. Angles of attack of $0°$ and $10°$ are considered. More details are given in [4]. The mesh has 5 different levels. The

coarsest level, or level 0, has a grid spacing of $\Delta x_0 = 0.01C$, where C is the chord length. The finest level is located around the airfoil and its grid spacing is $\Delta x_4 = C/1600$, which results in a maximal normalized wall distance y^+ of approximately 12. Dynamic mesh adaptation is used for mesh level 3 with a criteria based on the vorticity magnitude. The mesh has approximately $52 \cdot 10^6$ cells and simulations are run on 360 AMD processors (2.25GHz) at the Archer2 HPC facility with 26 hours wall-time needed to compute a single flow-over time C/U_∞.

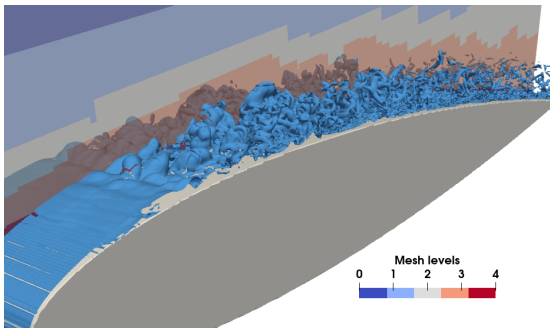

Figure 1: Iso-surface of the instantaneous magnitude of the vorticity. NACA0012 airfoil at 10° AoA.

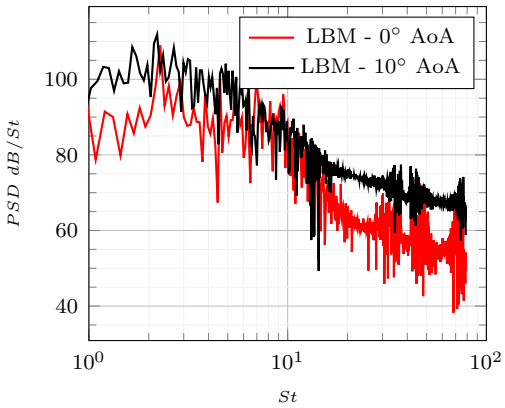

Figure 2: PSD computed from pressure signal at a pressure probe located $0.95C$ above the trailing edge.

Iso-surfaces of the magnitude of the instantaneous vorticity vector are displayed in Fig. 2; a plane in the z-direction visualizes the levels of mesh adaptation. Note how the adaptive mesh closely follows the vortices generated above the upper surface of the airfoil. We then compute the power spectral density (PSD) from a pressure probe data and compare scenarios with angles of attack of 0° and 10°, Fig. 2. PSD levels with an angle of attack of 10° are above the levels with 0° angle of attack for $\mathrm{St} < 7$ and $\mathrm{St} > 10$. The increased flow separation and vortices creation close to the leading edge in the 10° case increases the noise level on most of the observable spectrum by 10 dB to 20 dB.

Although possible, wall-resolved LBM-LES-AMR simulations at moderately high Reynolds number require considerable computational resources. To reduce the cost of our approach and extend the Reynolds number range, a boundary layer model has been implemented and its validation for a 2D airfoil is presented afterwards.

3 2D Airfoil - Wall model

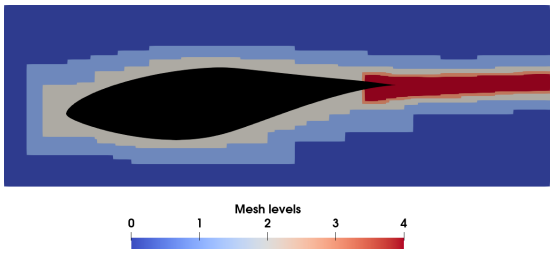

Figure 3: Mesh levels around the S809 airfoil at $-5°$ angle of attack.

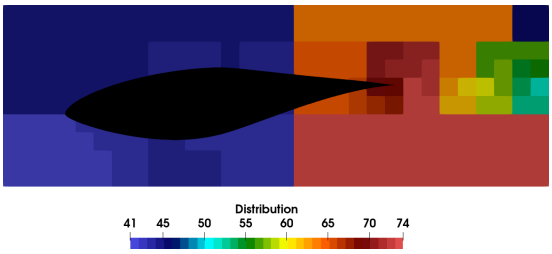

Figure 4: Cells distribution around the S809 airfoil at $-5°$ angle of attack.

The boundary layer model proposed by Maeyama *et al.* [1] is used here. The model enforces zero wall-normal velocity at the wall location along with a correct wall shear stress. The model achieves the blending of the RANS viscosity, produced by the wall model, with the subgrid-scale viscosity from the LES model. The airfoil chosen for this study is the S809 profile, proposed and studied experimentally in [5]. It is here simulated at angles of attack of $-5°$ and $9.22°$, at a Mach number of 0.1 and a Reynolds number, based on the chord length, of $2,000,000$. The domain is $22C$ long in the x- and y-direction. The AMR is used with 5 levels. The finest level is used around the trailing edge and in the close wake, with a mesh spacing of $C/1168$. For the rest of the airfoil, the grid spacing is $C/292$. The wake further downstream of the airfoil is refined at spacings of $C/292$ and $C/146$. Adaptive mesh refinement is used in the wake of the airfoil with a criteria based on the vorticity magnitude, cf. Fig. 3. The AMR algorithm re-grids the wake every $4.0 \cdot 10^{-3} C/U_\infty$. The mesh has $2,729,500$ cells on average and simulations are run on 256 AMD processors (2.25GHz). Cells are distributed among processors using a space-filling curve algorithm with rigorous domain decomposition. Figure 3 shows the distribution in the airfoil vicinity. It took approximately 300 wall-time seconds to simulate C/U_∞.

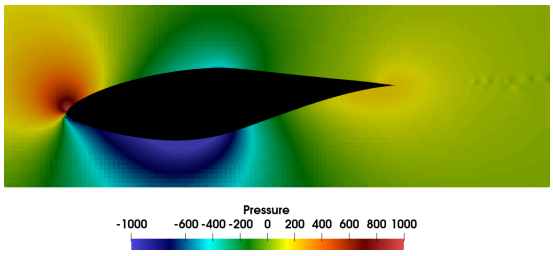

Figure 5: Close-up on the instantaneous pressure field for the simulation of the S809 airfoil at $-5°$ angle of attack.

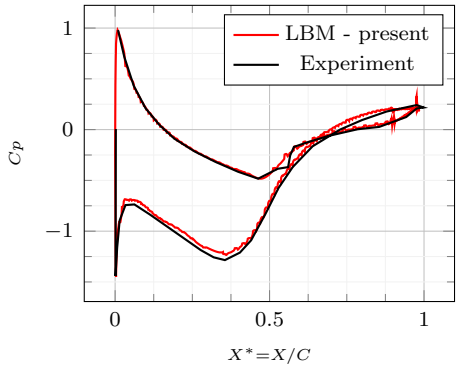

Figure 6: Pressure coefficient of the S809 arfoil at $9.22°$ AoA.

The averaged dimensionless mesh size over the airfoil surface is approximately $\Delta x^+ = 280$. The instantaneous pressure field is visible in Fig. 3. No influence from the mesh interface is visible and the AMR machinery is working smoothly. Pressure fluctuations can be observed downstream of the airfoil and are caused by the wake becoming unstable and generating vortices.

The time-averaged pressure coefficient along the airfoil surface for the angle of attack of $9.22°$ is given in Fig. 6. Our results are in good agreement with experimental data. Small discrepancies and fluctuations can be observed near the trailing edge. Indeed, the flow there is unsteady and our time-averaged sampling might be insufficient. However, even though we are using a finer mesh near the trailing edge, this edge is extremely sharp and a singularity still exists. Further mesh refinement would likely improve the predictions of our model here.

For the angle of attack of $-5°$, the error on the lift coefficient is found to be 0.89%. It is 0.6% for the $9.22°$ case. Our simulations are thus in excellent agreement with the experimental study of Somers [5]. This accuracy would not have been achievable without the AMR increasing the resolution of the mesh around the trailing edge and in the near wake.

4 CONCLUSIONS

Our LBM-LES-AMR software AMROC has been used to run 3D wall-resolved aeroacoustic simulations. To improve its capability, a boundary layer model for the Cartesian ghost-cell approach intrinsic to AMROC has been implemented. The flow around a 2D airfoil at high Reynolds number was then successfully predicted using this later capability. It has also been shown that this model is compatible with our adaptive mesh refinement machinery. In the near future, we intend to extend the boundary layer model to a 3D implementation and use it for aeroacoustic applications.

REFERENCES

[1] H. Maeyama, T. Imamura, J. Osaka and N. Kurimoto, "Turbulent channel flow simulations using the lattice Boltzmann method with near-wall modelling on a non-body-fitted Cartesian grid," *Computers and Mathematics with Application*, vol. 93, pp. 20–31, 2021.

[2] O. Malaspinas, *Increasing stability and accuracy of the lattice Boltzmann scheme: recursivity and regularization*, 2015.

[3] O. Malaspinas and P. Sagaut, "Consistent subgrid scale modelling for lattice Boltzmann methods," Journal of Fluid Mechanics, vol. 700, pp. 514-542, 2012.

[4] M. Grondeau and R. Deiterding, *Direct Prediction of Flow Noise Around Airfoils Using an Adaptive Lattice Boltzmann Method*, Handbook of Wind Energy Aerodynamics, 1-25, in press.

[5] Dan M. Somers, *Design and Experimental Results for the S809 Airfoil*, National Renewable Energy Laboratory, 1997.